Improved Estimation of Evolutionary Spectrum based on Short Time Fourier Transforms and Modified Magnitude Group Delay by Signal Decomposition

H K Lakshminarayana, J S Bhat and H M Mahesh

Abstract—A new estimator for evolutionary spectrum (ES) based on short time Fourier transform (STFT) and modified group delay function (MGDF) by signal decomposition (SD) is proposed. The STFT due to its built-in averaging, suppresses the cross terms and the MGDF preserves the frequency resolution of the rectangular window with the reduction in the Gibbs ripple. The present work overcomes the magnitude distortion observed in multi-component non-stationary signals with STFT and MGDF estimation of ES using SD. The SD is achieved either through discrete cosine transform based harmonic wavelet transform (DCTHWT) or perfect reconstruction filter banks (PRFB). The MGDF also improves the signal to noise ratio by removing associated noise. The performance of the present method is illustrated for cross chirp and frequency shift keying (FSK) signals, which indicates that its performance is better than STFT-MGDF (STFT-GD) alone. Further its noise immunity is better than STFT. The SD based methods, however cannot bring out the frequency transition path from band to band clearly, as there will be gap in the contour plot at the transition. The PRFB based STFT-SD shows good performance than DCTHWT decomposition method for STFT-GD.

Keywords—Evolutionary Spectrum, Modified Group Delay, Discrete Cosine Transform, Harmonic Wavelet Transform, Perfect Reconstruction Filter Banks, Short Time Fourier Transform.

I INTRODUCTION

IN general, signals like speech, seismic, biomedical signals (EEG, ECG), communication signals (frequency shift keying, radar returns involving Doppler shift, etc.) and communications over time varying channels (interference excision, channel modeling and equalization) display some form of non-stationary characteristics [1],[2]. It is often advantageous to display a non-stationary signal over a joint time frequency (TF) plane using TF signal representation methods [3]. For non-stationary signals, it is intuitively clear that its spectral properties change with time and, hence, a meaningful representation of these spectral properties must depend on a time variable. Thus, we look for a time –

H K Lakshminarayana is with the Department of Electronics, Kuvempu Uiversity, Shankarghatta, Shimoga, Karnataka,577 451, INDIA. (e-mail: lakkysharmahk@rediffmail.com).

J S Bhat is with the Physics Department, Karnatak University , Dharwad, 580 003, INDIA (e-mail: js_bhat@hotmail.com).

H M Mahesh is with the Department of Electronics Science, Jnana Bharathi, Banglore University, Banglore, (corresponding author: Mahesh HM , phone: +91   08022961361; fax: +91   08022961361; e-mail: hm_mahesh@rediffmail.com).

dependent power spectrum of the form $Sx(t, f)$ with S being a TF function of x, and t & f indicate the time and frequency, respectively. The short time Fourier transform (STFT), Wigner Ville distribution (WVD) and evolutionary spectrum (ES) are the techniques generally employed for the time-dependent spectral analysis.

It has been shown that the evolutionary periodogram (EP), STFT and a class of bilinear distribution (BD) are estimators of ES [2],[4][5]. In the case of STFT, due to built-in time domain smoothing, there are no cross terms and the spectrogram, the magnitude square of the STFT ensures the positivity of time–frequency spectral representation. However, with the STFT there is an uncertainty between time and frequency resolutions. The EP also produces positive spectra without any cross terms and for a given number of expansion functions, the data length controls the resolution of EP. Thus, the STFT is similar to EP; therefore in the rest of the paper we emphasis only on STFT than EP. Further, for a given window length, the STFT achieves best frequency resolution when the window is rectangular but suffers from Gibbs ripple due to abrupt truncation of signal. The use of any window other than rectangular though reduces the Gibbs ripple but only at the cost of frequency resolution [6],[7]. Thus the STFT can become a better estimator of ES, if the Gibbs ripple can be reduced without affecting the frequency resolution of the rectangular window.

For the spectral estimation, a modified group delay function (MGDF) has been proposed [7] - [10]. In the case of a signal obtained as output from a system, the MGDF removes the noise effect from the signal, which can be due to input and/or the one added at its output (observation noise). Further, for a signal associated with white noise, the MGDF improve the signal to noise ratio (SNR) without additional filtering. The MGDF has also been used to remove the Gibbs ripple without using any common window function and hence preserves the frequency resolution of the rectangular window [6],[11],[12]. In the transfer functions, zeros close to the unit circle introduce white noise to signal. The MGDF basically removes these zeros without disturbing the poles of the system/signal and hence preserves the frequency resolution [8, 10], but in special cases like multi amplitude and/or multi-component signals like cross chirp signals with different amplitudes, it shows magnitude distortion.

World Academy of Science, Engineering and Technology
International Journal of Electronics and Communication Engineering
Vol:3, No:11, 2009

In this paper we have proposed an improved estimator of evolutionary spectrum based on signal decomposition with DCTHWT or perfect reconstruction filter banks (PRFB). The STFT -GD with signal decomposition (SD) is used to reduce the magnitude distortion of improved STFT-GD. The SD based improved STFT performance is studied with DCT-HWT or PRFB. The improved readability of the TF representation is observed in the results of the present work. The application of the present work is demonstrated in interference modeling for non-stationary jamming noise in Direct Sequence Spread Spectrum (DSSS).

II. TIME-FREQUENCY REPRESENTSTION

Fourier transform (FT) assumes that the spectral characteristics of a signal do not change with time and hence it is not appropriate for the analysis of non-stationary signals. To get the information about spectral characteristics at different times the time–frequency representations (TFR) came into picture. This representation gives a natural description for the non-stationary signals. Indeed, TFRs characterize signals over a TF plane. They combine time-domain and frequency domain analyses to yield a potentially more revealing picture of the temporal localization of a signal's spectral components. The STFT is the first step in this direction and the bilinear distributions and evolutionary spectrum have evolved later.

A. Short time Fourier transform

The linear time–frequency representation STFT $X(n,\omega)$ of a signal $x(n)$ at time n and frequency ω is defined as

$X(n,\omega) = \sum_{k=0}^{N=1} h[k-n]x[k]e^{-j\omega k}$,where h [.] is a window function centered about zero.

The STFT gives the spectral information of the signal within the window at its position. By sliding the window $h[n]$ to different positions it is possible to get the time-varying spectral characteristics of the signal. However, STFT assumes that the signal is stationary within the length of the window. To better localize the signal characteristics in time, the window length has to be reduced. But, this results in a poor frequency resolution. Hence there is a tradeoff between frequency and time resolution [2]. Further, the use of a rectangular window that provides best possible frequency resolution suffers from Gibbs ripple. Hence to overcome the Gibbs ripple it is necessary to use common window functions like Hamming or Hanning. However, use of such window functions reduces the frequency resolution depending upon the smoothness of the window. For a given window, the frequency resolution can be improved only by increasing the window length but at the cost of time resolution. The squared magnitude of the STFT of the signal x[n] is given by

$$\hat{S}_{STFT}(n,\omega) = \frac{1}{N}\left|\sum_{k=0}^{N-1} h[k-n]x[k]e^{-j\omega k}\right|^2 . \tag{1}$$

B. Evolutionary spectrum

The evolutionary spectrum for the nonstationary signal analysis was introduced by Priestly and according to this; it is the set of bandpass filter with output powers computed by averaging the squared output samples in time [16]. But the Wold–Cramer evolutionary spectrum considers a nonstationary signal x[n] as the output of a linear time-varying (LTV) system driven by a stationary white noise [6], given by,

$$x[n] = \int_{-\pi}^{\pi} H(n,\omega)e^{-j\omega n} dZ(\omega) \cdot \tag{2}$$

Where $Z(\omega)$ is a process with orthonormal increments and $H(n,\omega)$ is a process slowly varying in time

The Wold–Cramer ES is given by

$$\hat{S}_{EP}(n,\omega) = \frac{N}{M}\left|\sum_{i=0}^{M-1}\beta_i^*[n]\sum_{k=0}^{N-1}\beta_i[k]x[k]e^{-j\omega k}\right|^2 , \tag{3}$$

where $\{\beta[n]_i\}$ are a set of M expansion of functions, which are orthonormal over $0 \le n \le N-1$, N is the length of the signal $x[k]$. The frequency resolution of the EP is given by $2\pi M/N$. The data length determines the basic resolution, i.e, $2\pi/N$. Hence for a given number of basis functions, the frequency resolution can be improved by only increasing the data length [6].

The STFT has more resemblance to the EP compared to BD and can be used as an estimator of ES. The EP and STFT differ only in terms of window function, which decides the frequency resolution. The EP provides a better frequency resolution than STFT. Improving the frequency resolution of STFT can make it a better estimator of ES with rectangular window [7].

III. HARMONIC WAVELET TRANSFORM [20]

The wavelet transform (WT) of a signal is generally realized in time domain by a two-channel PRFB using a dyadic structure. Newland[20] introduced the HWT and this enables the wavelet/ wave packet implementation in the frequency domain. For a wavelet function $w(t)$, the WT coefficient $a(t)$ of a signal $x(t)$ is given by

$$a(t) = \int_{-\infty}^{\infty} x(\tau)w(t+\tau)d\tau \cdot \tag{4}$$

In terms of Fourier transform,

$$A(\omega) = X(\omega)W^*(\omega),$$
$$a(t) = F^{-1}[X(\omega)W^*(\omega)]. \tag{5}$$

World Academy of Science, Engineering and Technology
International Journal of Electronics and Communication Engineering
Vol:3, No:11, 2009

Thus, the WT coefficients can be computed using FFT algorithm by Eq. (5) using $X(\omega)$ with $W(\omega)$ for different wavelet functions. Specifically, for the HWT of Newland [20], $W(\omega)$, is very simple and it is zero except over a finite band $[\pi / p, \pi / q]$, where p, q can be real numbers, not necessarily integers. The multiplication of $X(\omega)$ by $W^*(\omega)$, while using the discrete Fourier transform (DFT), is equivalent to grouping of the DFT coefficients of a signal in a dyadic fashion. The inverse DFT of each group yields harmonic wavelet transform coefficients (HWC) [20]. The inverse HWT can be achieved by deriving the complete DFT by proper concatenation of the DFT coefficient groups obeying the possible DFT conjugate symmetry and taking its inverse DFT. For HWT, the above choice of $W(\omega)$, though compact in the frequency domain, is of infinite duration in time domain. This can be overcome by using a proper smoothing weighing function for the grouped DFT coefficient sequence.

A. DCT harmonic wavelet transform (DCTHWT)

The harmonic wavelet transform based on DFT (DFTHWT), as already explained, has the features of simplicity with its built-in decimation and interpolation operations. The Fourier coefficients, which are already affected by leakage, are grouped. The processing on any band will affect the neighboring bands indirectly as the leaked energy also gets processed. Therefore to utilize the features of the harmonic wavelet transform, it is necessary to reduce the leakage effects and in this direction, use of DCT instead of DFT is an important step. Compared to the DFT, the DCT has a better frequency resolution due to data extension and this enables DCT to resolve the closely spaced spectral components [11].

The DCT of a N point signal $x(n)$, $n = 0,1,....,(N-1)$ is defined as the DFT of a 2N point symmetrically extended signal y(n),

$$y(n)=\begin{cases} x(n), & 0 \le n \le N-1, \\ x(2N-1-n), & N \le n \le 2N-1, \end{cases} \quad (6)$$

where y (n) is even symmetric with respect to the point [N-(1/2)]. This leads to DCT and is given by

$$C_x(k)=\begin{cases} \sum_{n=0}^{N-1} 2x(n)\cos\dfrac{\pi k(2n+1)}{2N}, & 0 \le k \le N-1, \\ -C_x(2N-k), & N \le k \le 2N-1. \end{cases} \quad (7)$$

Here, the DCT has been derived from the DFT.

With the DFTHWT, in getting the decimated subband component signal and in signal reconstruction, the conjugate symmetry of the DFT has to be accounted. The component signals can also be complex. But with the DCTHWT as the coefficients are real and the symmetry is built-in, no conjugation symmetry operation is required. Thus the DCTHWT is simpler and provides better performance.

B. Design of Two channel perfect reconstruction filter Banks with Frequency masking approach [18]

A filter bank is a set of filters. The analysis bank often has low pass and high pass filters. This separates the input signal into frequency bands. Two channel filter banks are mainly designed using three methods, i.e. spectral factorization method, Cepstrum method and Frequency-Response Masking (FRM) approach. First two methods result in more computational complexity when the individual filters have narrow transition bands. This problem can be resolved by using the FRM approach [19]. One price to pay is overall delay.

In the FRM approach, the transfer function of the overall filter is expressed as

$$H(z)= G(z^L)F_0(z)+ G_C(z^L)F_1(z), \quad (8)$$

where $G(z)$ and $G_C(z)$ are referred to as the model filter and complementary model filter, respectively. The filters $F_0(z)$ and $F_1(z)$ are referred to as the masking filters which extract one or several passbands of the periodic model filter $G(z^L)$ and complementary periodic model filter $G_C(z^L)$, where L is the interpolation factor. For a low-pass filter, typical magnitude responses for the model, masking, and overall filters are as shown in Fig 1.
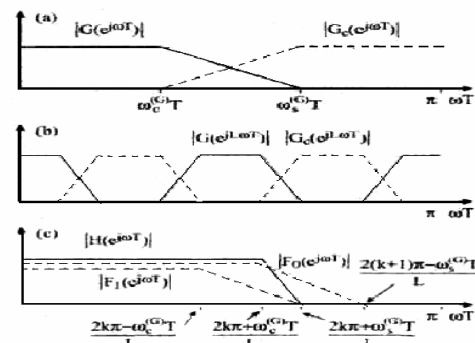

Fig. 1 Illustration of magnitude responses in the frequency-response masking approach.

The model filters $G(z)$ and $G_C(z)$ are odd-order linear-phase FIR filters with symmetric and anti-symmetric impulse responses, respectively, with $G_C(z)$ being related to $G(z)$ as $G_C(z)=G(-z)$. The filter $G(z)$ and $G_C(z)$ can be used to obtain two-channel filter banks with zero aliasing and arbitrary small magnitude distortion. The two masking filters $F_0(z)$ and $F_1(z)$ are linear-phase filters with equal delays. Both filters are consequently of either even or odd order and their impulse responses are symmetric since they must be able to realize both low pass and high pass filters.

If we use a non-linear phase filter in the analysis (synthesis) filter bank we need to use another filter in the

World Academy of Science, Engineering and Technology
International Journal of Electronics and Communication Engineering
Vol:3, No:11, 2009

synthesis (analysis) filter bank in order to make the overall distortion function a linear-phase function. A linear-phase filter can be obtained by cascading $H_0(z)$ and $H_1(z)$ as given by

$$H_0(z) = G(z^L)F_0(z) + G_C(z^L)F_1(z)$$
$$H_1(z) = G(z^L)F_0(z) - G_C(z^L)F_1(z) \quad \text{(9)}$$

In filter banks the analysis and synthesis filters are given by

$$
\begin{aligned}
H_{a0}(z) &= G(z^L)F_0(z) + G_C(z^L)F_1(z) \\
H_{a1}(z) &= G(z^L)E_0(z) + G_C(z^L)E_1(z) \\
H_{S0}(z) &= G(z^L)F_0(z) - G_C(z^L)F_1(z) \\
H_{S1}(z) &= G(z^L)E_0(z) + G_C(z^L)E_1(z),
\end{aligned}
\tag{10}
$$

where all of $H_{a0}(z), H_{a1}(z), H_{S0}(z)$ and $H_{S1}(z)$ belongs to the class of FRM FIR filters. In order to make the analysis/synthesis filters $H_{a0}(z)$ and $H_{a1}(z)$ $[H_{S0}(z)$ & $H_{S1}(z)]$ low pass and high pass filters, respectively, $F_0(z)$ and $F_1(z)$ must be low pass filters, whereas $E_0(z)$ and $E_1(z)$ must be high pass filters. $E_0(z)$ and $E_1(z)$ can be obtained by the relation, $E_0(z) = \pm F_1(-z)$ and $E_1(z) = \mp F_0(-z)$.

The analysis and synthesis filters make use of the same model and masking filters. The only difference is, in the synthesis filters, $F_1(z)$ and $E_1(z)$ are replaced with $-F_1(z)$ and $-E_1(z)$, respectively. The reason for this is, the distortion function then has a linear phase since both $H_{a0}(z), H_{S0}(z)$ and $H_{a1}(z), H_{S1}(z)$ are all linear-phase filters.

Given the pass band and stop band edges of $G(z)$, denoted here $\omega_C^{(G)}T$ and $\omega_S^{(G)}T$, respectively. We get pass band and stop band edges of $F_0(z)$ and $F_1(z)$ as

$$\omega_C T = \frac{2k\pi + \omega_C^{(G)}T}{L}, \quad \omega_S T = \frac{2k\pi + \omega_S^{(G)}T}{L} \tag{11}$$

and

$$\omega_C T = \frac{2k\pi - \omega_S^{(G)}T}{L}, \quad \omega_S T = \frac{2k\pi - \omega_C^{(G)}T}{L}, \tag{12}$$

respectively. Here k=(L-1)/4, only odd values of **L** are feasible since **k** is an integer. In the present case we have taken L=5.

IV. MGDF FOR COMPLEX SIGNALS [8],[3],[14]

The signal $x[n]$ is a minimum phase real signal with $X(\omega)$ as its Fourier transform,

$$\ln|X(\omega)| = \sum_{n=0}^{\infty} [c(n)\cos(\omega n)], \tag{13}$$

The GDF derived from the spectral magnitude is

$$
\begin{aligned}
\tau_p(\omega) &= -\frac{\partial}{\partial \omega}[\theta(\omega)] \\
&= \sum_{n=0}^{\infty} [nc(n)\cos \omega n].
\end{aligned}
\tag{14}
$$

Here, $\theta(\omega)$ is the unwrapped phase and $c(n)$ are cepstral coefficients. The cepstral coefficients are derived from magnitude information from (13). The GDF $\tau_p(\omega)$ is obtained using these coefficients and hence is called magnitude group delay (MGD).

The ripple/variance in a spectrum can be due to:
1) Signal truncation effect.
2) Associated white noise.
3) The input white noise that drives a system in generating the signal.
4) Any of the possible combinations.

These introduce zeros close to the unit circle. Application of a smoothing window to the signal, results in pulling the signal poles and zeros towards the origin in addition to the zeros near the unit circle. Hence the reduction in variance due to signal windowing is only at the cost of frequency resolution. The MGD modification given in [3] & [4] only removes the zeros close to the unit circle without disturbing the signal or system poles. Hence the use of modified MGD enables variance reduction preserving the frequency resolution of the rectangular window.

For a real signal $x(n)$, if $X(\omega) = N(\omega)/D(\omega)$, then $D(\omega)$ corresponds to the signal peaks and $N(\omega)$ mainly contributes to the ripples/variance [8],[3],[14]. Hence the ripple/variance of $X(\omega)$ can be removed by dividing it by $N(\omega)$. However, this may result in singularity problems. In the group delay domain, the same operation can be realized by multiplication avoiding any singularity. The MGD of $X(\omega)$, $\tau_p(\omega)$ is

$$\tau_p(\omega) = \tau_{pN}(\omega) - \tau_{pD}(\omega), \tag{15}$$

where $\tau_{pN}(\omega)$ and $\tau_{pD}(\omega)$ are the MGDs corresponding to $N(\omega)$ and $D(\omega)$ respectively. The group delay of signal $v(n)$ is given by

$$\tau_v(\omega) = \frac{V_R(\omega)Y_R(\omega) + V_I(\omega)Y_I(\omega)}{|V(\omega)|^2}, \tag{16}$$

where,

$y(n) = nv(n)$, $V(\omega) = FT[v(n)]$, $Y(\omega) = FT[y(n)]$. Further $V_R(\omega), Y_R(\omega)$ are the real and $V_I(\omega), Y_I(\omega)$ are the imaginary

World Academy of Science, Engineering and Technology
International Journal of Electronics and Communication Engineering
Vol:3, No:11, 2009

parts of $V(\omega)$ and $Y(\omega)$, respectively. Representing the numerator by $K(\omega)$, $\tau_v(\omega) = \dfrac{K(\omega)}{|V(\omega)|^2}$.

With this representation, (16) can be written as,

$$\tau_p(\omega) = \frac{K_N(\omega)}{|N(\omega)|^2} - \frac{K_D(\omega)}{|D(\omega)|^2}. \qquad (17)$$

For the simplicity of explanation, $K_N(\omega)$ and $K_D(\omega)$ can be considered as constants [10]. For zeros close to the unit circle, $|N(\omega)|^2$ will be very small and for signal poles which are relatively far from unit circle, $|D(\omega)|^2$ is large. Hence in (17), for $\tau_p(\omega)$, the contribution is mainly from the first term and this masks the signal peaks which are due to second term. This masking effect of these zeros can be reduced by multiplying $\tau_p(\omega)$ by $|N(\omega)|^2$. Hence, the modified MGD (MGDF) $\tau_{po}(\omega)$, becomes,

$$\tau_{po}(\omega) = K_N - \frac{K_D}{|D(\omega)|^2}|N(\omega)|^2. \qquad (18)$$

The estimate of $|N(\omega)|^2$, $|\hat{N}(\omega)|^2$ is given by [10],

$$\left|\hat{N}(\omega)\right|^2 = \frac{|X(\omega)|^2}{|\hat{X}(\omega)|^2} = \left[1 + \frac{|\Delta(\omega)|^2}{|\hat{X}(\omega)|^2}\right], \qquad (19)$$

and

$$\tau_{po}(\omega) = \tau_p(\omega)|\Delta(\omega)|^2 \qquad (20)$$

where $|\hat{X}(\omega)|^2$ is the smoothed power spectrum of the signal obtained by the truncated cepstral coefficient sequence and $\Delta(\omega)$ represents the fluctuating part of $X(\omega)$. For smoothed power spectrum $|\hat{X}(\omega)|^2$, the number of cepstral coefficients used should be sufficient to get only the gross feature of the spectrum. Selection procedure of number of cepstral coefficients are discussed in [3]. For a signal having flat spectral characteristic, in the GD $\tau_p(\omega)$ the contribution is only due to $\Delta(\omega)$. Therefore, to get a modified GDF $\tau_{po}(\omega)$ that is free from ripple on the flat floor, $\tau_p(\omega)$ has to be multiplied by $|\Delta(\omega)|^2$ [3], [8].

V. IMPROVED ESTIMATION OF EVOLUTIONARY SPECTRUM WITH STFT BASED ON SD BY DCTHWT/PRFB AND MGDF

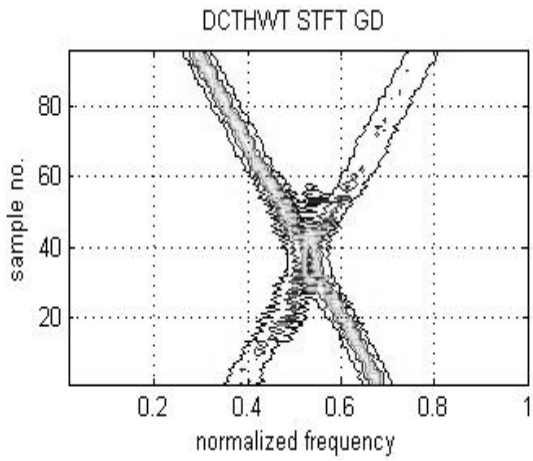The estimation of ES by STFT using a rectangular window shows better frequency resolution but, suffers mainly from ripple effect. One of the obvious solutions to remove the ripple effect is to use a smooth window function, which will smear the ripple effect and make the spectrum smooth. But this smoothness or reduction in the variance of the spectrum will reduce frequency resolution. Hence though the STFT is free from crossterms, it is not a good estimator of ES. Therefore, it is required to remove the ripple effect without any loss of frequency resolution. This is achieved by the application of MGDF [4].

In the proposed method, the multicomponent signal is decomposed into its components by DCTHWT /PRFB and their STFTs are computed. The Gibbs ripple in each STFT slice is reduced by applying the MGDF. The MGDF is applied for the fullband STFT [8]. Depending upon number of component present in the signal, fullband processing can be replaced by subband processing.
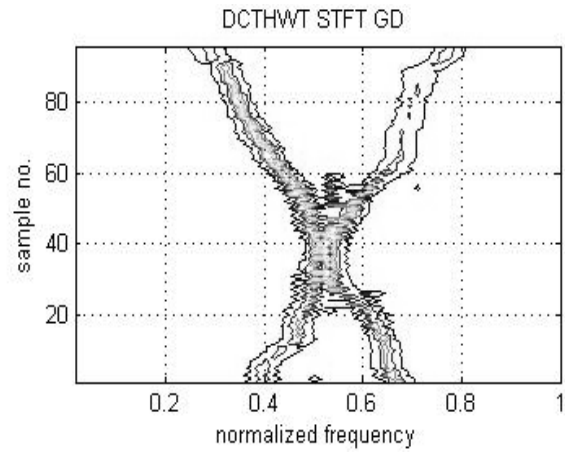
A. Improved estimation of evolutionary spectrum based on SD by DCT by MGDF processing in fullband (IFCTWVD).

After the decomposition of the signal, the STFT is computed with a rectangular window of suitable length and at each instant of time MGDF is computed. In STFT computation, autocorrelation coefficients for higher-order lags, derived from spectrogram, are made zero to reduce the variance and its FT is considered as an estimate of spectrogram. This estimate is supposed to be a positive quantity as it represents the power spectral density (PSD). However; the inevitable presence of the rectangular window may make the spectrogram values negative. Further, since the GDF $\tau_p(\omega)$ involves logarithmic operation as in (13) and (14), it is necessary to ensure that values of the slice of the spectrogram at each instant of time are positive. This is achieved by raising sufficiently the floor level by scaling up the autocorrelation coefficient at the zeroth lag. Further, in computing $\tau_p(\omega)$, the equivalent magnitude spectrum is
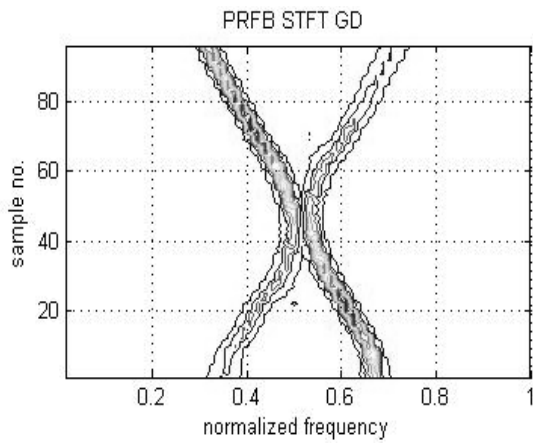

a)

World Academy of Science, Engineering and Technology
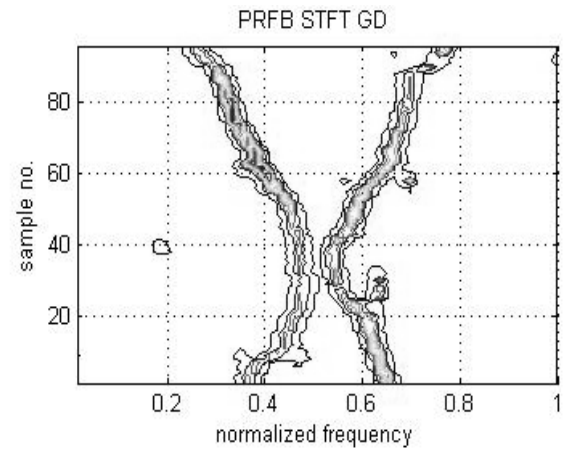International Journal of Electronics and Communication Engineering
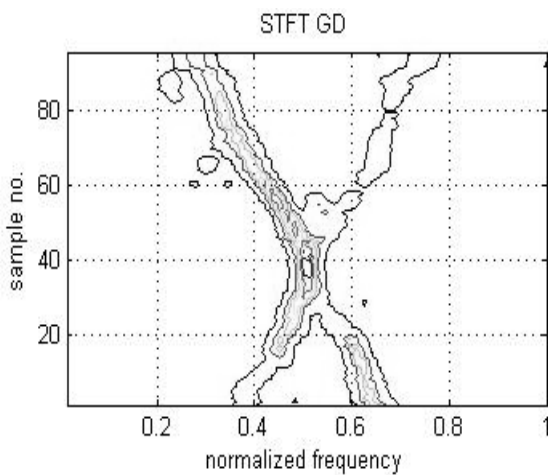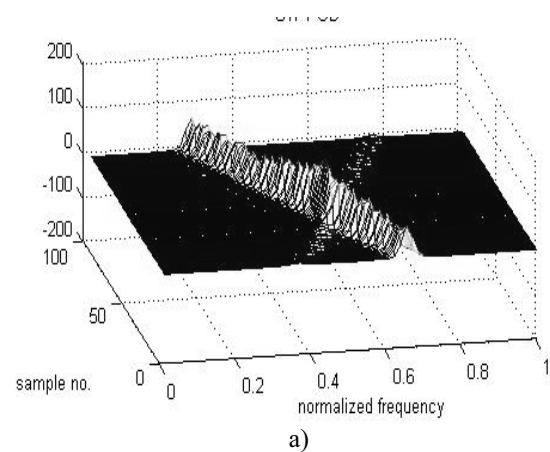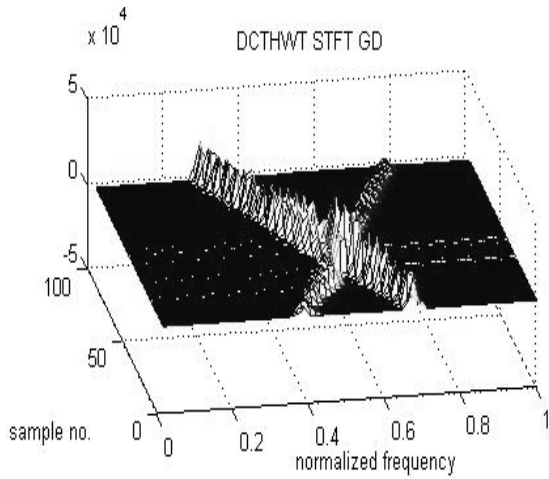Vol:3, No:11, 2009
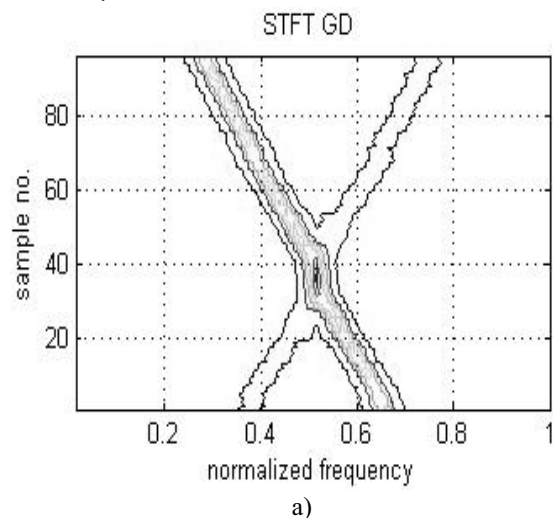
b)

e)

c)

f)

Fig. 2 Contour plots of STFT-GD (a),SD- STFT-GD with PRFB (b), SD-STFT-GD with DCT-HWT (c), for crossing chirp signals. Same plots with 3 dB noise (d, e & f).
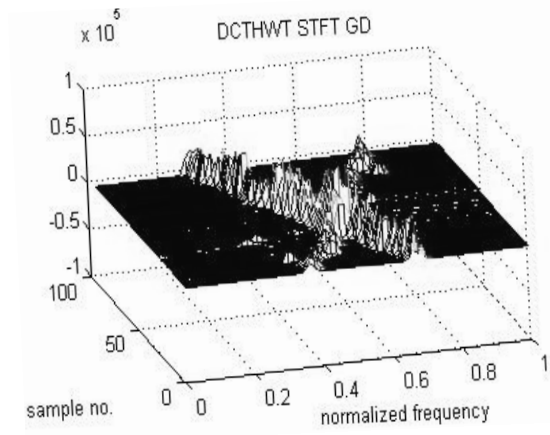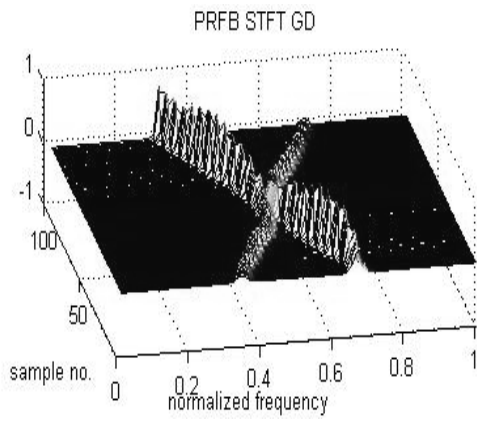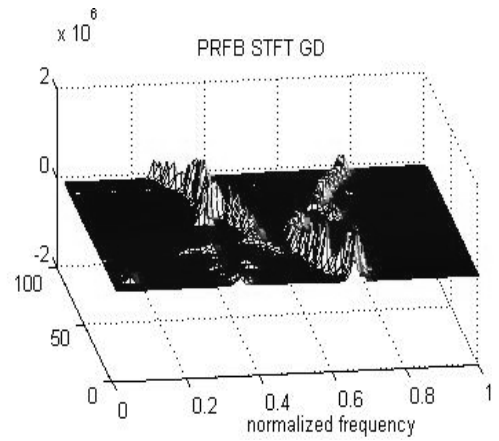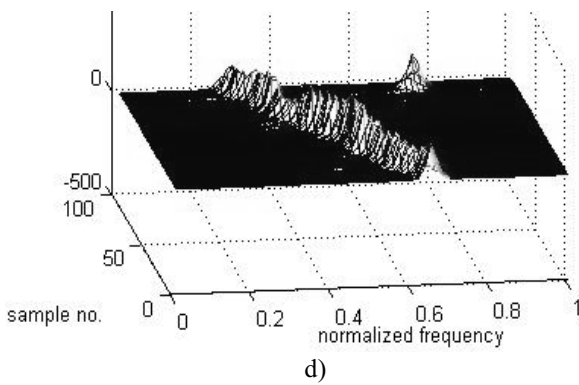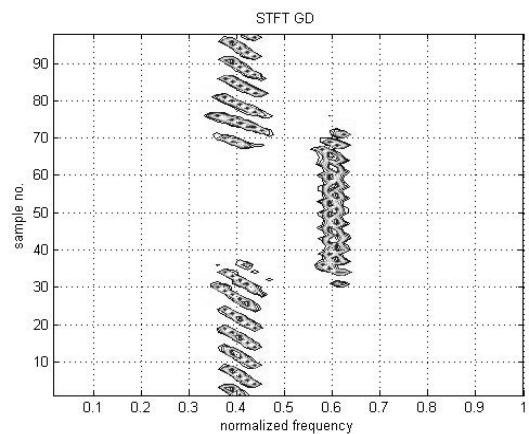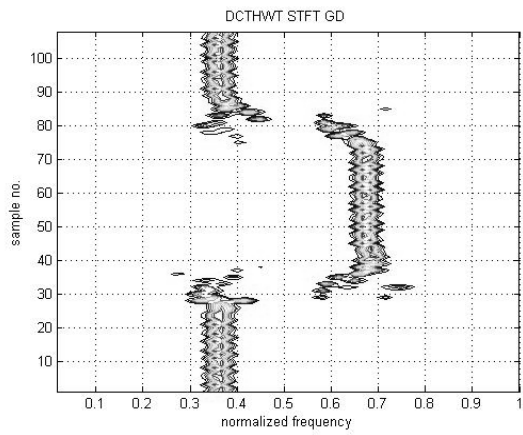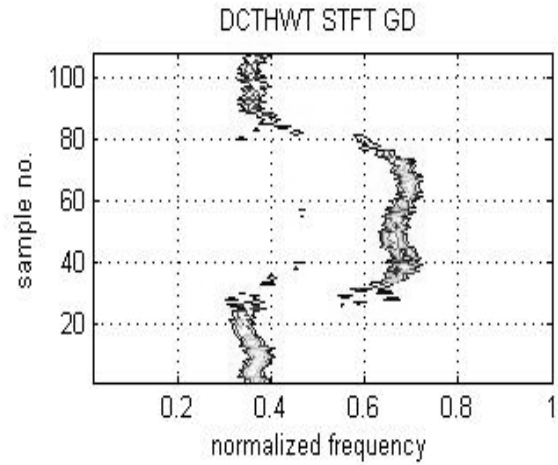

d)

a)

b)

e)

c)

f)

Fig. 3 Mesh plots of STFT-GD (a), SD- STFT-GD with PRFB (b), SD-STFT-GD with DCT-HWT (c), with cross chirp signals. Same plots for 3 db noise (d, e & f).
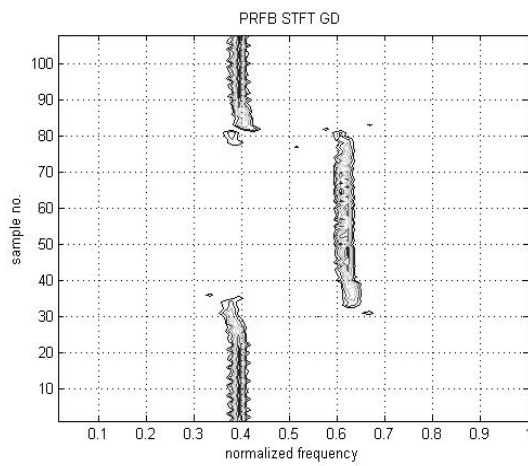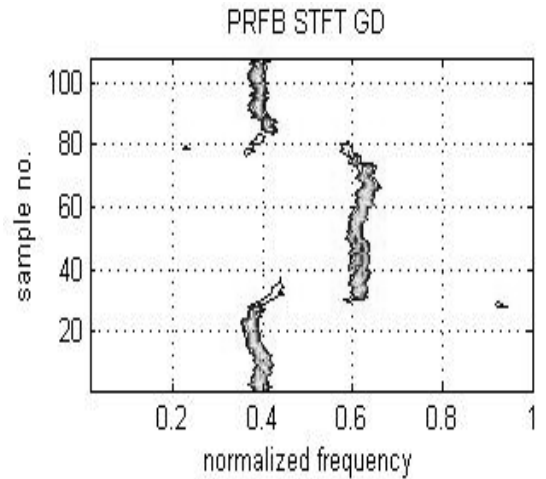

d)

a)

World Academy of Science, Engineering and Technology
International Journal of Electronics and Communication Engineering
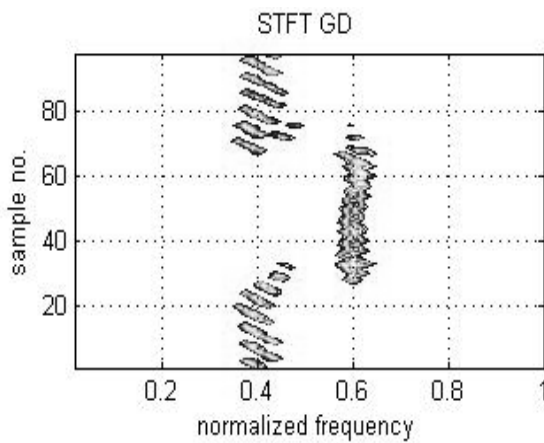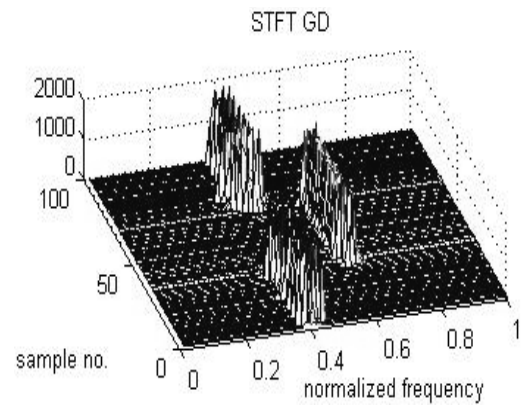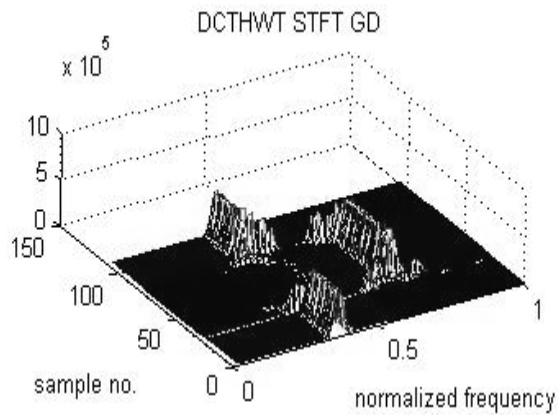Vol:3, No:11, 2009

b)

e)

c)

f)

Fig. 4 Contour plots of STFT-GD (a),SD- STFT-GD with PRFB (b), SD-STFT-GD with DCT-HWT (c),for FSK signal with 3 dB of FSK signal. Same plots with 3 db noise (d, e & f).
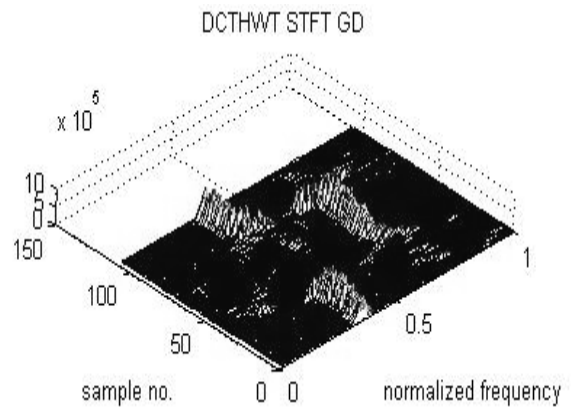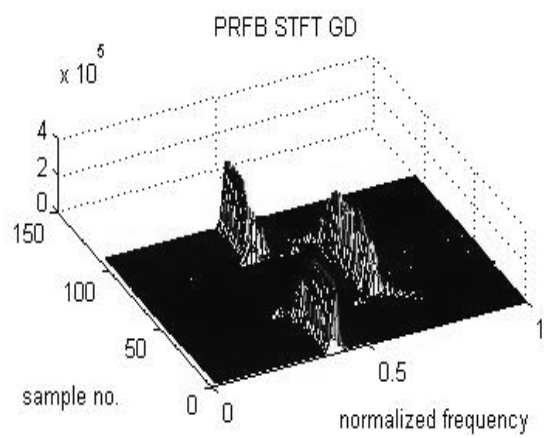

d)

a)

World Academy of Science, Engineering and Technology
International Journal of Electronics and Communication Engineering
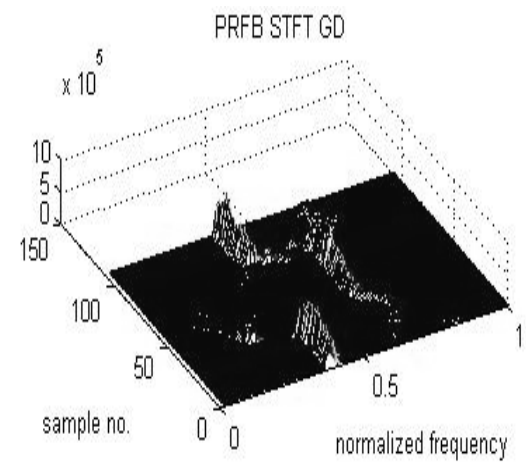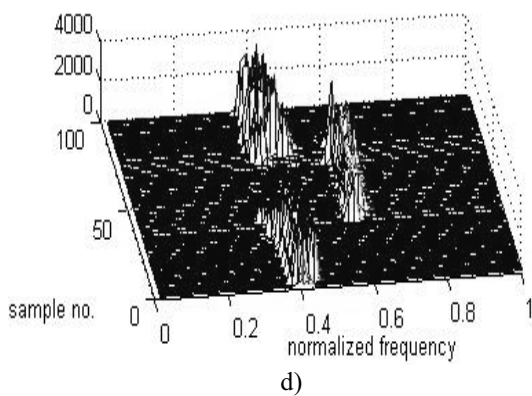Vol:3, No:11, 2009

b)

e)

c)

f)

Fig. 5 Mesh plots of STFT-GD (a), SD- STFT-GD with PRFB (b), SD-STFT-GD with DCT-HWT (c) , for FSK signal. Same plots with 3 dB noise (d, e, & f).

d)

World Academy of Science, Engineering and Technology
International Journal of Electronics and Communication Engineering
Vol:3, No:11, 2009

a)

b)
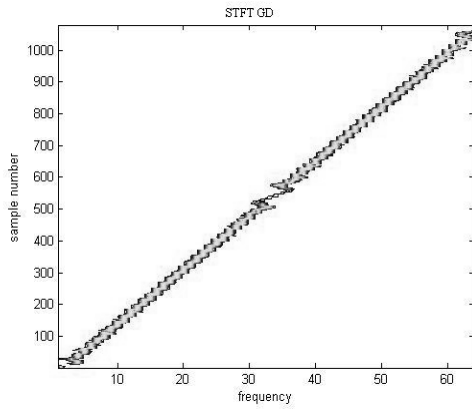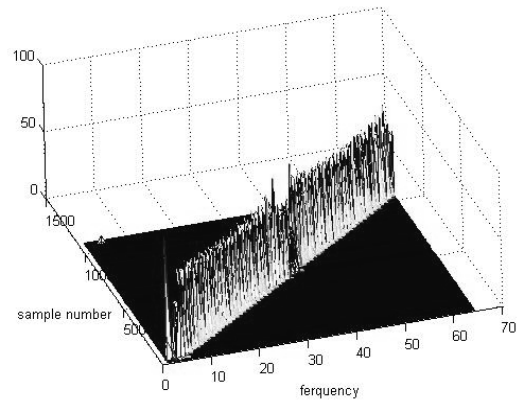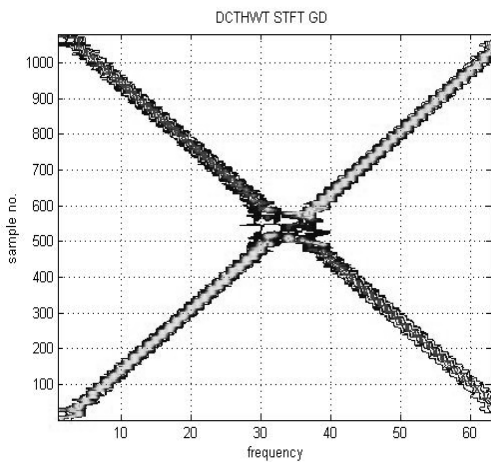
c)

Fig. 6 Contour plots of STFT-GD (a), SD-STFT-GD with DCT-HWT (b), SD- STFT-GD with PRFB (c) for nonstationary interference signal in DSSS.

a)

b)

c)

Fig. 7 Mesh plots of STFT-GD (a), SD-STFT-GD with DCT-HWT (b), SD- STFT-GD with PRFB (c), for nonstationary interference signal in DSSS.

World Academy of Science, Engineering and Technology
International Journal of Electronics and Communication Engineering
Vol:3, No:11, 2009

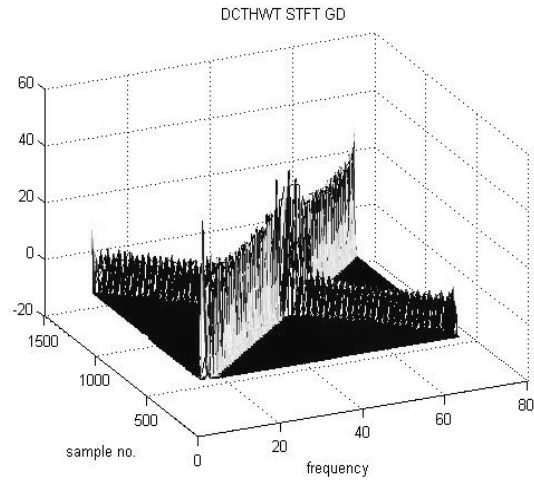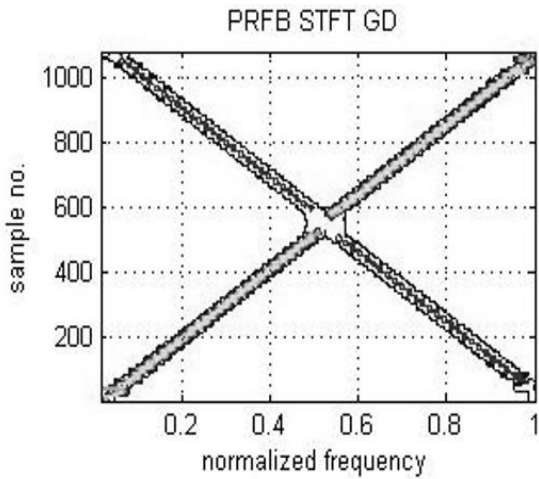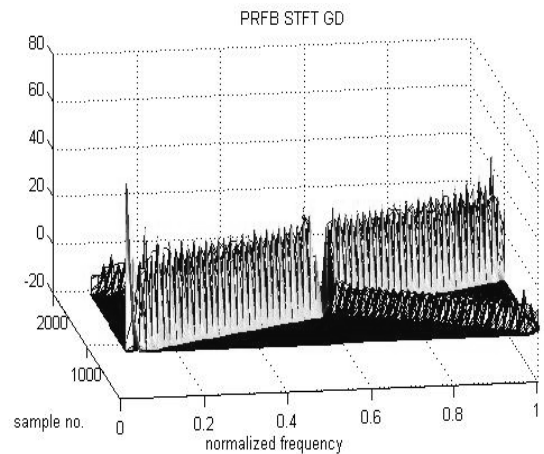computed from the spectrogram slice. To get back the TFR slice from GD function the gain and base level are adjusted with respect to the original log spectrum. For each TFR slice obtained from the MGDF, the original floor level is restored by subtracting its mean value and adding a scaled mean value (the scale factor being the same as that used in enhancing the autocorrelation at the zeroth lag). For deterministic signals like, cross chirps or frequency shift keying (FSK) signals, where only the Gibbs ripple on the floor is to be reduced, $\tau_p(\omega)$ is modified by multiplying with $|\Delta(\omega)|^2$. For a time varying random process, $|N(\omega)|^2$ function is used for computing modified $\tau_p(\omega)$.

B. Algorithm for the proposed improved ES Estimator

Step 1: Obtain the component signals with DCT HWT/PRFB as explained in Section III-A and III-B.

Step 2: Compute the FT of each truncated signal to get a component STFT slice and concatenating to get full STFT.

Step 3: At a particular instant $n = n_1$, compute the GD $\tau_p(l)$. For this, compute the definitely positive power spectral density: take inverse FT of the STFT slice and this gives complete IACR for that instant and raise the floor level of the STFT by multiplying the IACR zeroth lag value by which is much greater than unity (say 5000).

Step 4: Compute the MGDF $\tau_{po}(l)$ as mentioned in section IV, and get improved SD-STFT-GD slice.

Step 5: Compute the estimate of ES at time n_1: For this:

(i) Compute the sequence $s(k)$ from $\tau_{po}(l)$;

$$s_1(k) = IDFT\{\tau_{po}(l)\},$$

$$s(k) = \begin{cases} \dfrac{2s_1(k)}{k}, & k = 1,......N/2, \\ \dfrac{s_1(k)}{k} & k = N/2 \\ 0, & k = N/2+1,.....,N-1. \end{cases}$$

(ii) Compute $S(l)$: $\quad S(l) = \mathrm{Re}[DFT[s(k)]]$,

(iii) Obtain the normalized estimate $S_N(l)$ by scaling $S(l)$ with respect to $IM(n_1,l)$,

$$S_m(l) = S(l) - \frac{1}{N}\sum_{l=0}^{N-1} S(l),$$

$$A = \frac{1}{N}\sum_{l=0}^{R} IM(n,l), \quad and \quad IM_m(n_1,l) = IM(n_1,l) - A.$$

And R is the number of coefficients considered for gain and level adjustment

$$G = \max[S_m(l)]/\max[IM_m(n_1,l)],$$

$$S_N(l) = \frac{S_m(l)}{G} + A$$

(iv) The estimate of ES, $ES(n_1,l)$ is obtained from $S_N(l)$,

$$S1(l) = \exp[2S_N(l)], \quad and \quad B = \frac{1}{N}\sum_{l=0}^{N-1} S1(l)$$

$$ES(n_1,l) = S1(l) - B + \frac{B}{U}.$$

Step 6: Repeat steps 2 to 5 for each sample instant *n*, in the time interval considered and obtain the $ES(n,l)$ of single component signal.

Step 7: Concatenating the ES of different components to get the full *ES* in proper position.

VII. SIMULATION RESULTS

The performance of the proposed ES estimator will be illustrated for cross chirp signals (with different amplitude levels) and FSK signal. In all figures, the STFT-GD and STFT-GD with SD (with DCTHWT or PRFB) is illustrated with contour and mesh plots. The cross chirp signal is considered, i.e. given by

$$x(n) = A_1 \cos[2(566 - 1.6n)nT_s] + ...$$
$$............A_2 \cos[2(76\pi + 1.6n)nT_s]$$

For the proposed methods of ES estimation, in the case of crossing chirp signal with A_1=1 and A_2=0.5, and rectangular window of length 32 is used. The DFT length used is 256. The $|\Delta(\omega)|^2$ estimate is obtained by considering first 8 cepstral coefficients and lifting factor U=1000. The same parameters are used all STFT-SD illustrations. For designing of PRFB prototype filters $G(Z)$ and $G_c(Z)$, filter length 32 is considered and then it is interpolated with the factor L=5 to get $G(Z^L)$ and $G_c(Z^L)$. The anti-imaging filters are constructed with the length of 10. The resultant FRM based filter frequency response is illustrated in Fig. 1 that shows sharp cut-off.

The time–frequency contour and mesh plots for STFT-GD and for the proposed methods for two linear chirps are shown in Fig.2-3 (a, b & c) and for FSK signals are shown in Fig.4-5 (a, b & c), respectively. From the figures, the proposed ES is having better visibility/detectability and frequency resolution (in case of FSK) than that obtained with STFT-GD. In the proposed method two chirp signals are clearly visible, but in the STFT -GD method its magnitude is reduced. This indicates that the new ES is the generalization of STFT-GD. To bring out the performance of the algorithm in the presence of additive white Gaussian noise (AWGN) with SNR of 3 dB is considered, i.e. shown in Fig.2, 3, 4 and 5 (e, f & g). Here new algorithm shows better performance in noise suppression compared to STFT-SD.

For a FSK signal, the frequency resolution of the STFT–GD with SD is better than that of STFT-GD for lower window length. The frequency transition from one frequency to the other is better for STFT-GD but there is a smearing along the time axis indicating it has good frequency localization but

World Academy of Science, Engineering and Technology
International Journal of Electronics and Communication Engineering
Vol:3, No:11, 2009

poor time localization. In SD-STFT-GD achieves better time and frequency localization, which is also evident from the contour plot Fig. 4 (c).

A. Application to interference modeling in spread spectrum technique.

We finally apply our improved evolutionary spectrum to model the nonstationary multi-component interference in DS-SS signal, which helps in suppression of interference. The received signal is modeled as, $x(n) = s(n) + q(n) + w(n)$, where, $s(n) = \sum_k b_k c(n - KN_c)$ is the transmitted signal ($b_k \in \{-1,1\}$) are the transmitted bits and $c(n)$ is the length-N_c spreading sequence), $q(n)$ as a interference (jammer) signal and $w(n)$ as the white noise. Two *linear Frequency Modulated* (Chirp) signals with different amplitudes are considered as interference.

In order to model the interference, we simulated a spread – spectrum system with N_c =11 and SIR=-60db with neglecting noise. The signal length was 1100 with 100 data bits. The PRFB prototype filters are built with the parameters, window length 32 and frequency bins of 128. Also, final filter length of 32 is considered for PRFB.

The present technique has built in noise suppression capability; therefore it focuses only on the interference not on data components which act as a noise. The simulated results of the interference model are shown in Fig. 6 (a, b & c) with contour and Fig. 7(a, b & c) with mesh plots. This clearly indicates that, the SD based ES showed better detection of lower amplitude nonstationary signals and in SD PRFB showed good performance than DCTHWT technique.

VIII. CONCLUSION

A new Evolutionary Spectrum with improved performance based on signal decomposition (SD) by DCT- HWT / PRFB (with FRM approach) and MGDF processing in fullband is proposed. The DCTHWT is simple in computations, as compare to PRFB without FRM, but performance is better with PRFB. The FRM approach reduces the computational cost about 24% than earlier PRFB techniques and that makes it efficient for present approach. The proposed ES is applied to two linearly crossing chirps with different amplitude, FSK signal and same chirp signals as a non stationary interference signal in DS-SS communication are considered for performance measure. The result shows the better performance of the SD based ES with and without noise. They indicate that the detectability of low level component is high in SD based STFT–GD than STFT-GD. The frequency resolution even with noise is better than STFT-GD. The new algorithm for ES with STFT-GD and PRFB decomposition shows better performance than DCTHWT decomposition. In all the results of PRFB shows good detectability and in the crossing position than that of DCTHWT and the linearity in the frequency is clearer in PRFB case.

REFERENCES

[1] B. Boshash, "Time frequency signal analysis," in *Advances In Spectrum Analysis And Array Processing*, vol. 1, S. Haykin, Ed. NJ: Englewood Cliffs Prentice-Hall, 1991.

[2] L. Cohen, "Time-frequency distribution - a review," in July *1989 Proc. IEEE* , vol.77-7, pp. 941–981.

[3] S. V. Narasimhan, S. Pavanalatha, "Estimation of evolutionary spectrum based on short time Fourier transform and modified group delay*," Signal Processing,* vol.84, pp. 2139–2152. 2004.

[4] S. V. Narasimhan, A. R. Haripriya, B. K. Shreyamsha Kumar, "Improved Wigner–Ville distribution performance based on DCT/DFT harmonic wavelet transform and modified magnitude group delay ," *Signal Processing,* vol. 88, pp. 1–18, 2008.

[5] G. Matz and F. Hlawatsch, "Linear Tme-Frequency Filters: Online Algorithms and Applications", in *Applications in time frequency signal processing*, A. Papandreou - Suppappola, Ed., Boca Raton FL: CRC press, 2002.

[6] A. S. Kayhan, A. El-Jaroudi, L. F. Chaparro, "Evolutionary periodogram for nonstationary signals," *IEEE Trans. Signal Process.* Vol. 42 pp. 1527–1536, June 1994.

[7] C. S. Detka, A. El-Jaroudi, L. F. Chaparro, "Relating the bilinear distributions and the evolutionary spectrum," in 1993, *Proc.ICASSP'93 IV* pp. 496–499.

[8] S. V. Narasimhan, "Improved instantaneous power spectrum performance: a group delay approach," *Signal Processing,* vol. 80, pp. 75–88. 2000.

[9] S. V. Narasimhan, E. I. Plotkin, M. N. S. Swamy, "Power Spectrum Estimation of Complex Signals and its Application to Wigner–Ville Distribution: A Group Delay Approach," *Sadhana, Part-1, Indian Academy of Sciences, Bangalore, India,* vol. 23, pp. 57–71. February 1998.

[10] A. Hema Murthy, B. Yegnanarayana, "Speech processing using group delay functions," *Signal Processing*, pp.259–267. 1991

[11] S. V. Narasimhan, E. I. Plotkin, M. N. S. Swamy, "Power spectrum estimation of complex signals: a group delay approach," *Electron. Lett*, vol. 35, pp. 2182–2184. December 1999.

[12] B. Yegananarayana, A. Hema Murthy, "Significance of group delay functions in spectrum estimation"*, IEEE Trans Signal Processing*, vol. 40, pp. 2281–2289, Sept. 1992.

[13] M. B. Nayak, S. V. Narasimhan, "Autoregressive modeling of the Wigner–Ville distribution based on signal decomposition and modified group delay," *Signal Processing*, vol. 84, pp. 407–420, 2004.

[14] S. V. Narasimhan, M. B. Nayak, "Improved Wigner–Ville distribution performance by signal decomposition and modified group delay," *Signal Processing*, vol.83, pp. 2253–2538, 2003.

[15] S. V. Narasimhan, S. Pavanalatha, "Estimation of evolutionary spectrum based on STFT and modified group delay," *IEEE TENCOM—2003*, Bangalore, India, pp.1198–1203.

[16] M. B. Priestly, "Power spectral analysis of nonstationary random processes," *J. Sound Vib*. vol. 6 –I, pp. 86–97, 1967.

[17] M. Sansal, A. S. Kayhan, "IF and GD estimation from evolutionary spectrum," *Signal Processing*, vol. 81, pp. 197–202, 2001.

[18] P. P. Vaidyanathan, *Multirate systems and filter banks.* Pearson, 2006, ISBN 81-7758-942-3, ch. 6.

[19] L. Zhang, Y. Lian, and C. C. Ko, "A new approach for design sharp FIR filters using frequency masking technique," in *DSP Workshop,* Oct. 2000.

[20] D.E. Newland, "Wavelet analysis of vibration, Part-1: theory*," J. Vib. Acoust. Trans. ASME 116,* pp. 409–416, 1994.

Haegoppa Krishnasharma Lakshminarayana was born in the year 20th june, 1982 in Sagar, Karnataka, India. He received the Master of Science in electronics degree from "Kuvempu university", Karnataka,India in 2005.

He is currently pursuing PhD in Digital Signal Processing under the guidance of Dr. H M Mahesh and co-guidance Prof. J S Bhat , Kuvempu University and Karnataka University, Dharwad respectively. His research interest includes Digital Signal Processing, Time frequency Analysis, Signal Processing for communication especially in Spread Spectrum technique and image processing.